

# Gap size dependent transition from direct tunneling to field emission in single molecule junctions

Dong. Xiang, Yi. Zhang, Feliks Pyatkov, Andreas. Offenhäusser, and Dirk. Mayer \*

**The judgment of directly tunneling and field emission:** An appropriate model for the description of the current-voltage behavior of tunneling junctions was given by Simmons *et al.* The Simmons equation assumes a trapezoidal barrier when the applied bias is smaller than the barrier height. In the zero-bias limit the barrier is rectangular and the Simmons equation reduces to  $I \propto \exp(-2d\sqrt{2m\phi}/\hbar)$ , where  $d$  is the barrier width (here, the gap between the nanoelectrodes),  $m$  represents the electron effective mass, and  $\phi$  is the barrier height which can be approximated by the energy offset between the Fermi level of the nanoelectrode and the nearest molecular orbital. As an opposite limit one can consider the case when the applied bias exceeds the barrier height. For this assumption, the electron transport mechanism will change from direct tunneling to field emission transport (Fowler-Nordheim tunneling), and the Simmons equation can be written as  $\ln(I/V^2) \propto -\frac{4d\sqrt{2m\phi^3}}{3\hbar q}(\frac{1}{V})$ . In the field emission regime,  $\ln(I/V^2)$  depends linearly on  $1/V$  for a fixed gap size.<sup>[1]</sup>

**Self-assembly of molecules on the gold surface:** The target molecules were integrated between the nanoelectrodes by a self assembly process to generate a metal/molecules/metal junction. For this purpose, 1 mM ethanolic solution of 1,8-octanedithiol (ODT), a molecule which contains two thiol

termini as binding groups, was prepared in a protective atmosphere where the oxygen level was less than 1 ppm. A 10  $\mu\text{L}$  droplet of this solution was placed on the junction area under argon atmosphere. After a self-assembly period of five minutes on the gold surface of the electrodes, the sample was thoroughly rinsed with ethanol and dried in a nitrogen stream.

**Junction fabrication:**

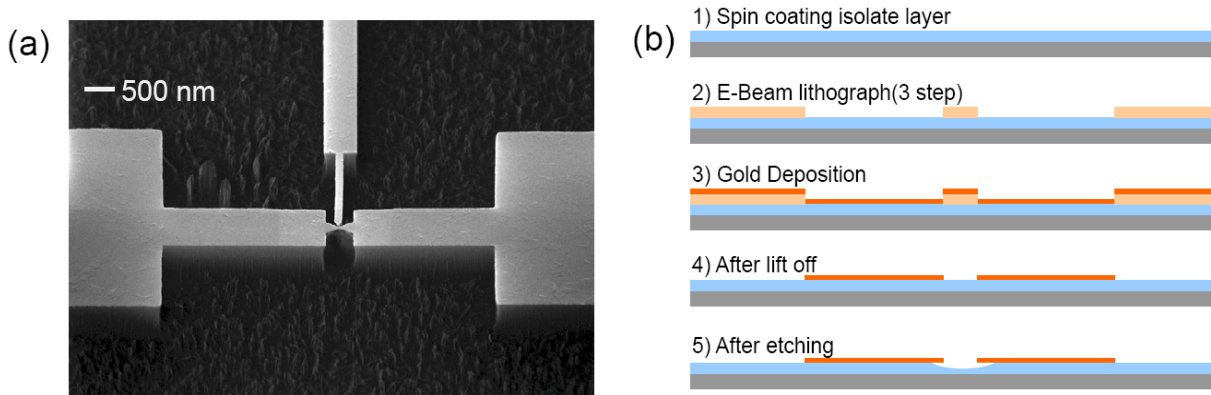


Figure S1 (a): Top view SEM picture of the nanoelectrode chip. Figure S1(b): Side view of the chips fabrication process, which consist of five steps 1-5. 1) A polyimide layer (HD-4000, HD Microsystem) about 3  $\mu\text{m}$  thick, is spun on the substrate. After baking it at 200 °C for 20 minutes, the substrate was annealed for one hour at 300 °C at a pressure of 10<sup>-3</sup> mbar. 2) The e-beam lithography process consists of three separate steps. First, 200 nm of the positive tone resist (PMMA, Polymethylmethacrylate 649.04 from ALLRESIST) was spun onto the substrate and baked at 180 °C for 2 minutes. Second, the electrode pattern was written by means of a Leica Vistec EBPG-5000 plus lithography System. Finally, a standard development procedure was applied by inserting the substrate into development solution (ALLESIST AR 600-55) for about 50 seconds, then the substrate was transferred into 2-propanol to stop the development. 3) After the development, the resist layer serves as a mask for the metal deposition. At this step, 2 nm Ti and

40 nm Au are deposited on the substrate surface in a vacuum chamber by e-beam evaporation.<sup>4)</sup> After deposition of the metals, the sample is immersed in acetone for lift off.<sup>5)</sup> In the final step, the polyimide is isotropically dry etched to obtain a suspended metal bridge. This is done by reactive on etching (RIE) at the following conditions: 32 sccm of oxygen and 8 sccm of CHF<sub>3</sub> and a power of 100 W.<sup>[2]</sup>

### ***Calibration of attenuation factor:***

The distance between the two electrodes for both the opening and the closing direction was controlled by bending or relaxing the substrate, respectively. An attenuation factor of  $r = \Delta x / \Delta z \approx 5 \times 10^{-6}$  ( $\Delta x$  is the gap distance change,  $\Delta z$  is the push rod displacement) was determined for the used setup, which implies that the distance between the nanoelectrodes was controllable with sub Ångstrom accuracy.

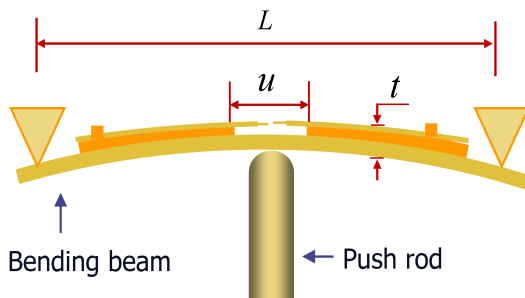


Figure S2 (a): Schematic drawing of the break junction setup. The attenuation factor is defined by the geometrical configuration of the system. According to previous reports, it can be calculated as:  $r = \Delta x / \Delta z \approx 6ut / L^2$ .<sup>[3]</sup> Here,  $r$  is the attenuation factor;  $u$  is the length of the suspend bridge;  $t$  is the thickness of the steel substrate;  $L$  is the length between the two outer posts.

For our device we obtained:

$$r = \Delta x / \Delta z \approx 6ut / L^2 \approx 6 \times 900\text{nm} \times 0.22\text{mm} / 20\text{mm} \times 20\text{mm} \approx 6 \times 10^{-6}$$

The attenuation factor can be furthermore determined from  $I(d)$  dependence of bare metal tunneling junction.

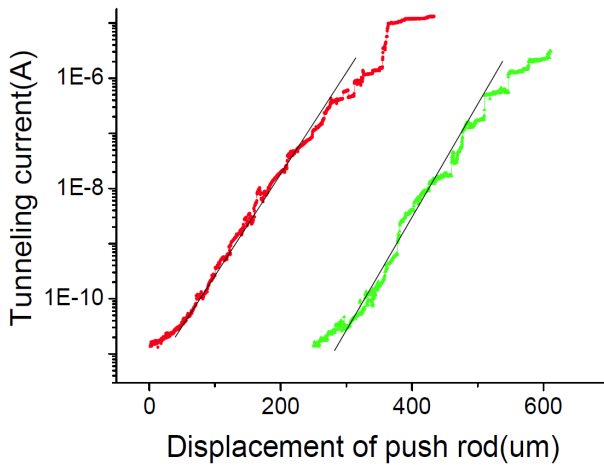


Figure S2 (b): Determination of the attenuation factor from the change of tunneling current as a function of the displacement of the push rod.

At low bias voltages the tunneling current can be described by the following equation:

$$I \propto \exp(-2d\sqrt{2m\phi} / \hbar) \quad (1)$$

Here,  $d$  is the gap size,  $m$  is the electron effective mass,  $\phi$  is the barrier height. Equation (1) can be written as:

$$I \propto \exp\left[-1.02d\sqrt{\phi}(eV)^{-0.5} A^{-1}\right] \quad (2)$$

For  $\phi_B$  of a bare gold junction in air, a value of 2.0 eV can be assumed.<sup>[3]</sup> According to equation 2, a change of the tunneling current by one order of magnitude will require a displacement

of the nanoelectrodes of  $\Delta d \approx 1.5 \text{ \AA} \approx \Delta x$ . From the slope of the measured  $I(d)$  curves, one can determine the displacement of the push rod  $\Delta z \approx 30 \mu\text{m}$  needed to obtain the corresponding current change, see Figure S2b. Thus, the attenuation factor can be calculated from the ratio of the two lengths:  $r = \Delta x / \Delta z = 1.5 \text{ \AA} / 30 \mu\text{m} = 5 \times 10^{-6}$ . This value corresponds well with the result obtained from the geometrical estimation, see Figure S2 (a).

***Contribution of direct tunneling between gold electrodes:***

Direct tunneling has to be considered as well to explain the enhanced field emission for narrow electrode gaps. However, in our case  $V_T$  shifts in a bias window between 0 V and  $\pm 1$  V. M. L. Trouwborst and co-workers demonstrated in Reference 4 that  $V_T$  falls within a range between 1.4 V and 2.2 V if direct tunneling was dominate in Au–vacuum–Au junctions. In their publication it was shown that the  $I/V$  curves have an almost linear shape for biases below 1V and turn into S-shape at biases above  $V_T$  (higher 1.4V). Therefore, we believe that a contribution from direct tunneling between the electrodes is leading to a rather linear increase of the tunneling current within the investigated bias regime (0V to 1V) and cannot explain the observed strong nonlinear increase of the  $I/V$  curves for the molecule containing junctions, manifested in  $V_T$  below 1V.

***Adjustment of the number of molecules entrapped in the junction at a given gap size:*** The experiments were performed in a way that we first established a stable junction. The junction conductance should be in the range of single molecule conductance (known from literature). At this stage, the position of the push rod was noted. Starting from this configuration we recorded  $I/V$  curves and altered afterwards the gap size by pushing the electrodes closer together (approximately by 6 Å to 10 Å). After releasing the junction to the original gap size, an additional  $I/V$  characteristics was recorded. This procedure was repeated until the junction collapses or jumps to

contact ( $G > 1G_0$ ). During each approaching and withdrawing process there was a certain probability that either new bonds between molecules and electrodes were formed or existing bonds were broken. Therefore, it can be assumed that the two nanoelectrodes were bridged by different numbers of molecules after this procedure, although the final gap size was nearly the same. Finally, the  $I/V$  curves were analyzed. After analyzing the data one can estimate how many molecules were bridging the junction. The main assumption here is, that the  $I/V$  response with lowest conductance corresponds to a single molecule junction.

***Reproducibility of junction formation:***

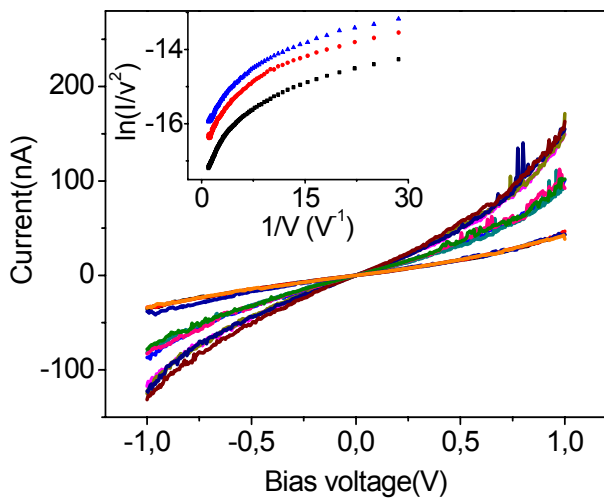


Figure S3: Additional exemplary  $I/V$  curves of metal/ODT/metal junctions at fixed gap size recorded from a different sample. The junctions were assembled as described before. By this method of approaching and withdrawing the nanoelectrodes, molecular junctions with different number of trapped molecules but similar final gap sizes were obtained. Almost all the  $I/V$  measurements fall down to three sets of curves. The sets represent multiples (1, 2, 3) of the (fundamental) characteristic of a single molecule junction. This kind of experiments can be

reproduced by several different samples, however the actual  $I/V$  characteristics might deviate to some extent from sample to sample. Each sample has an unique arrangement of atoms and molecules, which leads to a certain variation of the tunneling response, however the  $\ln(I/V^2)$  versus  $1/V$  characteristics remains unaffected. The insert picture shows the  $\ln(I/V^2)$  versus  $1/V$  presentation, which demonstrates that no field emission was observed independent of the number of entrapped molecules.

**Electric field strength in nanogaps:**

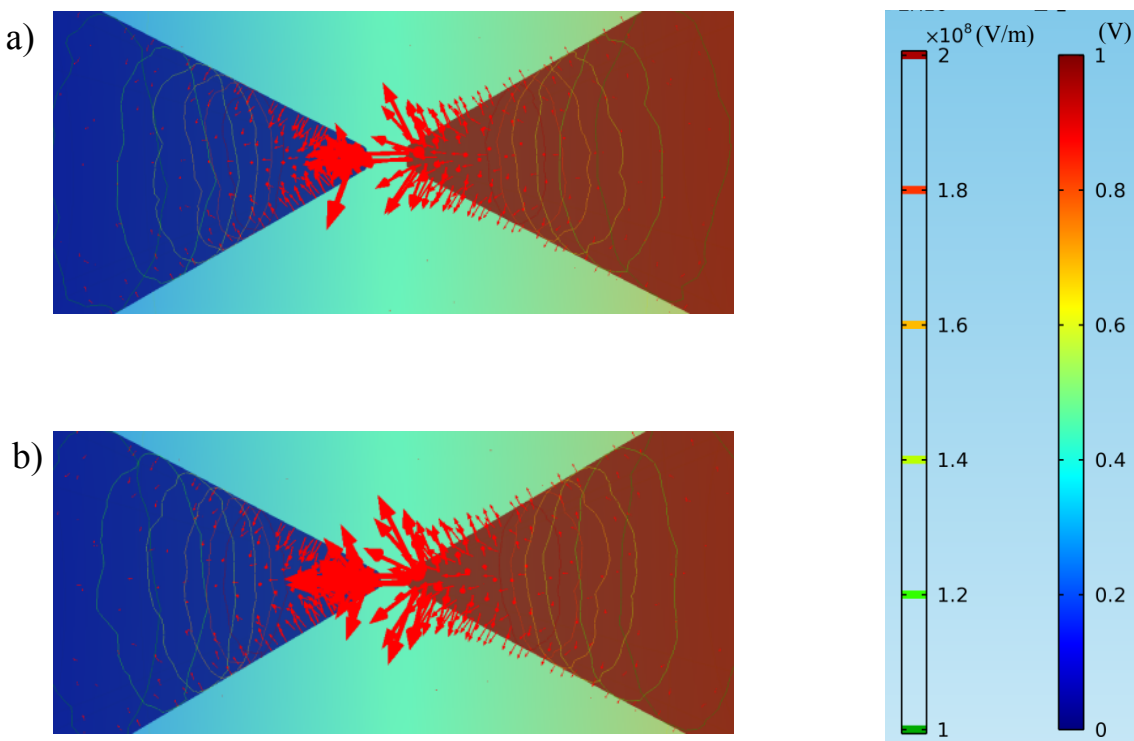


Figure S4: Simulation of the electrical field and potential distribution at two different gap sizes.

a) 1.2 nm and b) 0.8 nm gap size between the two nanoelectrodes. 1 V voltage was applied to the right nanoelectrode of a) and b) and the conjugated electrodes were connected to ground. The geometry of the electrodes is assumed as a cone: bottom radius 5 nm, top radius 0.25 nm, height

9.5nm. The arrow length in the picture is proportional to the electrical field strength (V/m). The contour shows the value of electrical field on the electrode surface. The simulation was done by COMSOL and demonstrates that a few angstrom change of the gap size results in a considerable alternation of the electrical field strength in the nanogap.

## References and notes

- [1]. J. M. Beebe, B. S. Kim, J. W. Gadzuk, C. D. Frisbie, J. G. Kushmerick, *Phys. Rev. Lett.*, 2006, **97**, 026801.
- [2]. L. Grüter, M.T. González, R. Huber, M. Calame, C. Schönenberger, *Small*, **2005**, 1, 1067-1070.
- [3]. C. Zhou, C.J. Muller, M.R. Deshpande, J.W. Sleight, M.A. Reed, *Appl. Phys. Lett.*, **1995**, 67, 1160-1162.
- [4]. M. L. Trouwborst, C. A. Martin, R. H. M. Smit, C. M. Guedon, T. A. Baart, S. J. van der Molen, J. M. van Ruitenbeek, *Nano Lett.*, DOI: 10.1021/nl103699t.